VSP

Journal of Biomaterials Science 21 (2010) 95–112

Journal of BIOMATERIALS SCIENCE
brill.nl/jbs

Local Delivery of Tobramycin from Injectable Biodegradable Polyurethane Scaffolds

Andrea E. Hafeman [a], **Katarzyna J. Zienkiewicz** [a], **Erin Carney** [b], **Brandon Litzner** [b], **Charles Stratton** [b], **Joseph C. Wenke** [c] **and Scott A. Guelcher** [a,*]

[a] Department of Chemical Engineering, 2301 Vanderbilt Place, VU Station B #351604, Vanderbilt University, Nashville, TN 37235, USA

[b] Department of Pathology, Vanderbilt University, Nashville, TN 37232, USA

[c] US Army Institute of Surgical Research, Brooke Army Medical Center, Fort Sam Houston, TX 78234, USA

Received 18 August 2008; accepted 31 December 2008

Abstract

Infections often compromise the healing of open fractures. While local antibiotic delivery from PMMA beads is an established clinical treatment of infected fractures, surgical removal of the beads is required before implanting a bone graft. A more ideal therapy would comprise a scaffold and antibiotic delivery system administered in one procedure. Biodegradable polyurethane (PUR) scaffolds have been shown in previous studies to promote new bone formation *in vivo*, but their potential to control infection through release of antibiotics has not been investigated. In this study, injectable PUR scaffolds incorporating tobramycin were prepared by reactive liquid molding. Scaffolds had compressive moduli of 15–115 kPa and porosities ranging from 85–93%. Tobramycin release was characterized by a 45–95% burst (tuned by the addition of PEG), followed by up to 2 weeks of sustained release, with total release 4–5-times greater than equivalent volumes of PMMA beads. Released tobramycin remained biologically active against *Staphylococcus aureus*, as verified by Kirby–Bauer assays. Similar results were observed for the antibiotics colistin and tigecycline. The versatility of the materials, as well as their potential for injection and controlled release, may present promising opportunities for new therapies for healing of infected wounds.

Keywords

Scaffold, polyurethane, biodegradable, sustained release, antibiotic, tobramycin, *Staphylococcus aureus*, local delivery

* To whom correspondence should be addressed. Tel.: (1-615) 322-9097; Fax: (1-615) 343-7951; e-mail: scott.guelcher@vanderbilt.edu

 DOI:10.1163/156856209X410256

Report Documentation Page

Form Approved
OMB No. 0704-0188

1. REPORT DATE	2. REPORT TYPE	3. DATES COVERED
01 JAN 2010	**N/A**	**-**

4. TITLE AND SUBTITLE	5a. CONTRACT NUMBER
Local delivery of tobramycin from injectable biodegradable polyurethane scaffolds	5b. GRANT NUMBER
	5c. PROGRAM ELEMENT NUMBER
6. AUTHOR(S)	5d. PROJECT NUMBER
Hafeman A. E., Zienkiewicz K. J., Carney E., Litzner B., Stratton C., Wenke J. C., Guelcher S. A.,	5e. TASK NUMBER
	5f. WORK UNIT NUMBER
7. PERFORMING ORGANIZATION NAME(S) AND ADDRESS(ES)	8. PERFORMING ORGANIZATION REPORT NUMBER
United States Army Institute of Surgical Research, JBSA Fort Sam Houston, TX 78234	
9. SPONSORING/MONITORING AGENCY NAME(S) AND ADDRESS(ES)	10. SPONSOR/MONITOR'S ACRONYM(S)
	11. SPONSOR/MONITOR'S REPORT NUMBER(S)

12. DISTRIBUTION/AVAILABILITY STATEMENT
Approved for public release, distribution unlimited

13. SUPPLEMENTARY NOTES

14. ABSTRACT

15. SUBJECT TERMS

16. SECURITY CLASSIFICATION OF:			17. LIMITATION OF ABSTRACT	18. NUMBER OF PAGES	19a. NAME OF RESPONSIBLE PERSON
a. REPORT	b. ABSTRACT	c. THIS PAGE			
unclassified	**unclassified**	**unclassified**	**UU**	**19**	

1. Introduction

Open fractures resulting from orthopaedic trauma often allow bacteria into the wound, which can cause osteomyelitis and compromise fracture healing [1–5]. Contamination must be treated immediately to allow proper healing. Local delivery of antibiotics can achieve high local concentrations while systemic levels remain low. This approach is a common clinical practice and has been demonstrated in animal studies to be safe and effective for treating osteomyelitis [6–12].

Local delivery of tobramycin from implanted poly(methyl methacrylate) (PMMA) cement beads is an established therapy for treating infected fractures, but only a small amount (<10%) of the drug is released [10, 13–16]. The PMMA beads are not resorbable and must be surgically removed after 2–6 weeks, at which time a bone graft is implanted to aid healing [14]. An ideal therapy for such infected fractures would include both a delivery system and a scaffold to promote fracture healing. The system would release the antibiotic dose over an extended period of time, biodegrade to non-cytotoxic decomposition products at a rate comparable to that of tissue healing, and support ingrowth of cells and new tissue. Calcium sulfate pellets impregnated with antibiotic (Osteoset T, Wright Medical) have been shown to be effective in treating osteomyelitis in animals and humans [6, 17–19]. These biomaterials are biodegradable and osteoconductive, but calcium sulfate can be associated with seromas and drainage problems [19]. Sustained release of tobramycin encapsulated in poly(D,L-lactic-co-glycolic acid) (PLGA) biodegradable microspheres has also been reported over a period of up to four weeks, and the released tobramycin is biologically active *in vivo* [20].

Tissue-engineered scaffolds potentially offer advantages for controlled release of antibiotics by providing both sustained release of the bioactive component as well as a template for infiltration of new cells and tissue. Biodegradable polyurethanes (PURs) have been investigated extensively as scaffolds for tissue regeneration due to their potential for controlling the degradation rate and mechanical properties [21–27]. Scaffolds prepared from segmented PUR elastomers based on hexamethylene diisocyanate (HDI) have been shown to support ingrowth of cells and new bone formation and to degrade to non-cytotoxic decomposition products when implanted in the iliac crest of sheep [28, 29]. Other *in vivo* studies have demonstrated the potential of segmented PUR elastomers for regeneration of cardiovascular tissue [30–32].

In an alternative approach, PUR networks have been synthesized by two-component reactive liquid molding [24, 26, 33–35]. An advantage of reactive two-component systems is the potential to develop injectable scaffolds that can be combined with a biological, such as antibiotics or growth factors, prior to injection. Two-component foams with porosities >90% prepared from HDI and polyester triols supported mineralization *in vitro* [26]. However, these materials were cured at 60°C and are, therefore, not suitable for injection. In another study, a reactive putty comprising a lysine diisocyanate (LDI) prepolymer and calcium phosphate exhibited good integration with host tissue, fibrovascular penetration and in-growth

of vascular buds when implanted in rats [35]. However, the porosity and pore size of these materials was not reported, and scaffolds fabricated from LDI have been reported to have poor resilience [36].

PUR biomaterials have also been investigated as delivery systems. Biodegradable PUR scaffolds prepared from linear segmented elastomers were shown to support controlled release of bFGF, suggesting the potential utility of PUR scaffolds for drug delivery applications [37]. In another study, release of PDGF-BB from a reactive two-component PUR network was shown [36]. However, the bioactivity of the PDGF-BB released from the reactive PUR network was not investigated.

In this study, we report the release of biologically active tobramycin from reactive two-component PUR scaffolds. The materials have a working time of >3 min and cure at room temperature, thus rendering them suitable for injection. The effects of scaffold hydrophilicity and degradation rate on tobramycin release and bioactivity were investigated. Sustained release of tobramycin for up to two weeks was observed, and the biological activity of the released tobramycin was comparable to that of fresh material. The scaffolds exhibited porosities $>90\%$ and mechanical properties consistent with those of rubbery elastomers and leathery plastics.

2. Materials and Methods

2.1. Materials

Glycolide and D,L-lactide were obtained from Polysciences (Warrington, PA, USA), tertiary amine catalyst (TEGOAMIN33) from Goldschmidt (Hopewell, VA, USA), poly(ethylene glycol) (PEG, 600 Da) from Alfa Aesar (Ward Hill, MA, USA), and glucose from Acros Organics (Morris Plains, NJ, USA). Tobramycin was obtained from X-Gen Pharmaceuticals (Big Flats, NY, USA), and hexamethylene diisocyanate trimer (Desmodur N3300A) was a gift from Bayer Material Science (Pittsburgh, PA, USA). All other reagents were purchased from Sigma-Aldrich (St. Louis, MO, USA). Prior to use, glycerol and PEG were dried at 10 mmHg for 3 h at 80°C, and ε-caprolactone was dried over anhydrous magnesium sulfate, while all other materials were used as received [38]. Simplex P cement beads with tobramycin were obtained from Stryker (Mahwah, NJ, USA).

2.2. Polyurethane (PUR) Scaffold Synthesis

The 900-Da trifunctional polyester polyol was prepared from a glycerol starter and ε-caprolactone, glycolide, and D,L-lactide monomers at a ratio of 60:30:10 (T6C3G1L), and stannous octoate catalyst, as published previously [33, 39, 40]. PUR scaffolds synthesized from the T6C3G1L polyester triol have been previously reported to degrade to 65% of their initial mass after 18 weeks incubation time in PBS at 37°C [36]. These components were mixed in a 100-ml three-neck flask with mechanical stirring under argon for 36 h at 140°C. The polyols were then dried under vacuum at 80°C for 14 h. As shown in previous studies, the half-life of the

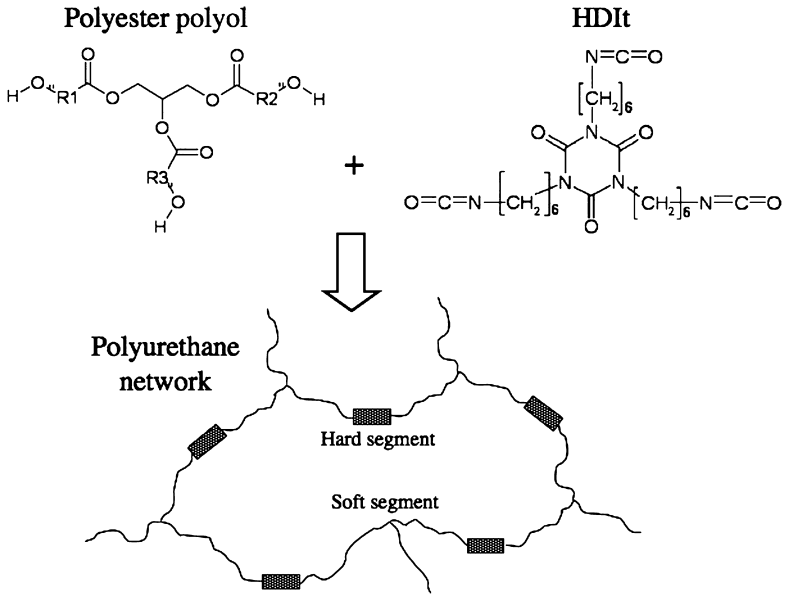

Figure 1. Synthesis of PUR networks.

polyester triol regulates the degradation rate of the PUR network in which they are incorporated [33, 36].

The PUR scaffolds were synthesized by reactive liquid molding of the aliphatic hexamethylene diisocyanate trimer (HDIt) and hardener [33, 39]. The hardener contained the polyol, 1.5 parts per hundred parts polyol (pphp) water, 4.5 pphp TEGOAMIN33 tertiary amine catalyst, 1.5 pphp sulfated castor oil stabilizer, 4.0 pphp calcium stearate pore opener, and when appropriate, 20 pphp lyophilized tobramycin (8 wt% of the final scaffold). The isocyanate was added to the hardener and mixed for 15 s in a Hauschild SpeedMixer™ DAC 150 FVZ-K vortex mixer (FlackTek, Landrum, SC, USA), for a targeted index (NCO:OH × 100) of 115. The resulting reactive liquid mixture then rose freely for 10–20 min. Some materials were synthesized with PEG (600 Da), such that the total polyol content consisted of 50 or 70 mol% polyester polyol with 50 or 30 mol% PEG. The basic reaction scheme for the PUR network synthesis is illustrated in Fig. 1.

Core densities were determined from mass and volume measurements of triplicate cylindrical foam cores, of 7 mm diameter × 10 mm height samples [41]. The core porosities (ε_C) were calculated from the density values (ρ_C), where $\rho_P = 1200$ kg/m^3 is the PUR specific gravity and $\rho_A = 1.29$ kg/m^3 is the specific gravity of air [33]:

$$\varepsilon_C = 1 - \left(\frac{\rho_C}{\rho_P}\right)\frac{(\rho_P - \rho_A\rho_P)/\rho_C}{\rho_P - \rho_A}.$$

Pore size distribution and interconnectivity were also assessed by scanning electron microscopy (Hitachi S-4200 SEM, Finchampstead, UK).

Tobramycin was added as a powder to the hardener prior to reaction with the triisocyanate resin in order to minimize its reactivity with the reactive two-component PUR. Tobramycin's five primary amino groups otherwise cause it to react rapidly with isocyanates when in solution [42]. Tobramycin is insoluble in polyester polyol, the primary component in the hardener; consequently the tobramycin remains in the solid phase during the chemical reaction. A loading of 8 wt% was chosen to approximate the level of tobramycin delivered from the equivalent volume of PMMA cement beads, but higher loading can be achieved if necessary.

2.3. PMMA Bead Synthesis

The PMMA cement beads were made according to the manufacturer's instructions. Briefly, the liquid monomer was added to the bone cement powder and hand mixed. The resulting paste was rolled into individual 50-mg beads, approx. 5 mm in diameter.

2.4. In Vitro *Release*

Triplicate 500-mg samples of the scaffolds each in 1 ml phosphate-buffered saline (PBS, pH 7.4) were mixed end-over-end while incubating at 37°C. At designated time points from 0.5 to 30 days, the buffer was removed from each vial and replaced. All release samples were frozen until analysis at the end of the 30 days. The released tobramycin was derivatized with *o*-phthaldialdehyde (PHT) and quantified with a Waters Breeze HPLC and UV detector, using a previously published method [43]. Of each sample, 250 µl was added to 100 µl PHT (100 mg/ml in methanol) and 150 µl isopropanol. This mixture was vortexed for 30 s and incubated at room temperature for 45 min before injection. The injected sample (50 µl) was separated in an XTerra reverse-phase guard column (C8 5-µm 3.9 × 20 mm) and XTerra reverse-phase column (C18 5-µm 4.6 × 250 mm) and analyzed at 333 nm. The mobile phases were as follows: (A) 0.1% acetic acid in water and (B) 88.5% acetonitrile in water with 0.1% acetic acid. Both were filtered through a 0.2 µm filter and degassed under vacuum. The buffer ratio was 80:20 (A/B) for the first 2 min, with a gradual gradient to 77:23 (A/B) from 2 to 6 min. The samples were calibrated by an external standard curve from 0.05 µg/ml to 30 µg/ml. With a 1.0 ml/min flow rate, the tobramycin peak eluted at approx. 6.5 min.

2.5. Antibiotic Biological Efficacy

The tobramycin activity was evaluated by Kirby–Bauer, or diffusion, assays. Colonies of methicillin-susceptible *Staphylococcus aureus* from the American Type Culture Collection (ATCC 25923) were suspended in trypticase soy broth and the turbidity was matched to a 0.5 MacFarland standard. The bacteria were then streaked onto Mueller–Hinton agar plates (lower limit of detection was 20 CFU/ml). Tobramycin scaffold samples were cut into discs (6 × 2 mm, 400–600 µg tobramycin per disc) and placed on the agar plates. Zones of inhibition (ZI) were measured in comparison with 10-µg tobramycin BBL SensiDiscs (BD, Franklin

Lakes, NJ, USA) and individual PMMA beads, with 3–4 mg tobramycin per bead, after incubation at 37°C for 24 h. The 10-μg tobramycin BBL SensiDiscs were chosen as a positive laboratory control, since this is a standard control used in pathology laboratories. Additionally, the bioactivity of the tobramycin after sustained release was evaluated. 0.5-μg tobramycin aliquots from release samples at 8, 20 and 30 days, as well as 0.5 μg pure tobramycin, were pipetted onto blank SensiDiscs. These discs were again placed onto *S. aureus*-streaked agar plates and the ZI were measured after 24 h.

2.6. Mechanical Properties

Dynamic mechanical properties of a representative selection of scaffolds, both with and without tobramycin, were measured in compression mode. Cylindrical 7×6 mm samples were compressed along the axis of foam rise. The temperature-dependent storage modulus and glass transition temperature (T_g) of each material were evaluated under a temperature sweep of -80 to $+100$°C, at a compression frequency of 1 Hz, 20-μm amplitude, 0.3% strain and 0.2 N static force. The stress relaxation modulus was evaluated as a function of time under 2% strain and 0.2 N static force. The frequency-dependent storage modulus was also evaluated by a frequency sweep of 0.1 to 10 Hz at a constant temperature of 37°C, with 0.3% strain and 0.2 N static force. Stress–strain curves were generated by controlled-force compression of the cylindrical foam cores at 37°C. With an initial force of 0.1 N, each sample was deformed at 0.1 N/min until it reached 50% strain (i.e. 50% of its initial height). The Young's (elastic) modulus was determined from the slope of the initial linear region of each stress–strain curve [44]. The scaffolds could not be compressed to failure due to their elasticity, so the compressive stress was measured at 37°C after 1 min at 50% strain in the DMA stress relaxation mode, as a measure of compressive strength [41]. Calculated from the measured force and cross-sectional sample area, the compressive stress indicates material compliance such that more compliant materials require lower stress to induce a particular strain.

2.7. Statistical Analysis

Statistical analysis of the results was performed using single factor analysis of variance (ANOVA). In cases where statistical significance is cited, the sample size is greater than or equal to three replicates per material.

3. Results

3.1. PUR Scaffold Characterization

The density and porosity of the PUR scaffolds with and without tobramycin are shown in Table 1. Incorporation of 8 wt% tobramycin in the PUR scaffolds increased the density (and therefore decreased the porosity), although not with statistical significance ($0.05 > P > 0.005$). In most cases, the addition of PEG had an insignificant effect on PUR density and porosity. However, the T6C3G1L-PEG50

Table 1.
Density, porosity and mechanical properties of PUR/tobramycin scaffolds

Material	Tobramycin	Density (kg/m^3)	Porosity (vol%)	T_g (°C)	Storage modulus at 37°C (kPa)	Young's modulus (kPa)	Compressive stress (kPa)
T6C3G1L-PEG0	+	139.7 ± 6.0	88.5 ± 0.5	41.3	1268	105.5 ± 16.1	67.9 ± 18.7
T6C3G1L-PEG0	−	98.2 ± 12.5	91.9 ± 1.0	40.3	723	114.5 ± 29.7	10.5 ± 1.0
T6C3G1L-PEG10	+	133.5 ± 21.4	89.0 ± 1.8	16.5	1059	99.4 ± 18.8	47.8 ± 7.4
T6C3G1L-PEG20	+	107.3 ± 12.2	91.2 ± 1.0	2.8	43	43.2 ± 5.2	12.0 ± 1.4
T6C3G1L-PEG30	+	118.6 ± 8.7	90.2 ± 8.9	7.5	152	41.2 ± 7.6	22.3 ± 6.6
T6C3G1L-PEG30	−	90.2 ± 2.6	92.6 ± 0.2	24.3	14.4	58.2 ± 14.9	6.6 ± 0.5
T6C3G1L-PEG50	+	176.9 ± 4.1	85.4 ± 0.3	8.8	28	48.2 ± 16.5	38.3 ± 9.7
T6C3G1L-PEG50	−	93.7 ± 11.4	92.3 ± 1.0	18.5	18.4	14.6 ± 2.7	6.7 ± 0.6

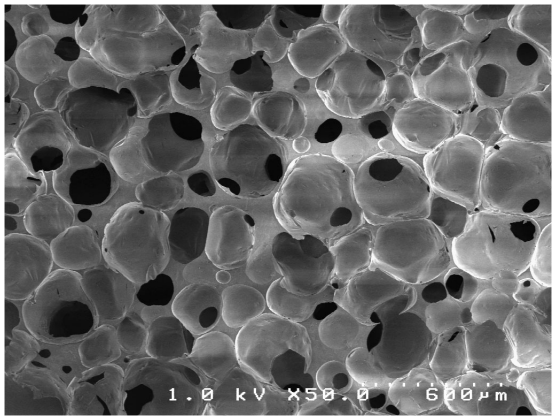

Figure 2. Scanning electron micrograph (SEM) of T6C3G1L-PEG0 scaffold.

scaffold with tobramycin exhibited a significantly higher density than any of the other materials. An SEM image of the T6C3G1L-PEG0 scaffold with 8 wt% tobramycin (Fig. 2) suggests an interconnected pore structure, which is supported by evidence from previous studies of cellular infiltration within the scaffold interstices [33, 36].

3.2. In Vitro *Release*

Tobramycin release profiles from the PUR scaffolds and PMMA beads are presented in Fig. 3. The burst release increased from 45% to 95% as the PEG content in the polyol component was increased from 0 to 50%. Interestingly, there was a significant increase in the burst release of tobramycin when the PEG content was elevated from 20% to 30%. As the PEG content increased, the amount of tobramycin released at later time points (after the initial burst) decreased from 35% of the total release to $<5\%$. Therefore, at the highest PEG content (50%), almost no additional antibiotic was released after the first 24 h. After 30 days, the total release of tobramycin ranged from 70 to 95%, with 30 and 50% PEG scaffolds demonstrating the highest cumulative release. In contrast, the total release of tobramycin from the PMMA cement beads after 30 days was 20%, with little additional release after 7 days. Tobramycin release is likely independent of material degradation. While the release profiles of the scaffolds containing 0, 30 and 50% PEG differed considerably, previous studies showed no statistically significant differences ($P > 0.05$) in the *in vitro* degradation rates of these scaffolds during the 4-week time period corresponding to the release experiments [36].

3.3. Antibiotic Biological Efficacy

While the data in Fig. 3 demonstrate that tobramycin is released from the PUR scaffolds, they do not address the question of whether the tobramycin is biologically active. Therefore, the bioactivity of the tobramycin released from the PUR scaffolds and PMMA cement beads over 24 h was assessed by the standard Kirby–

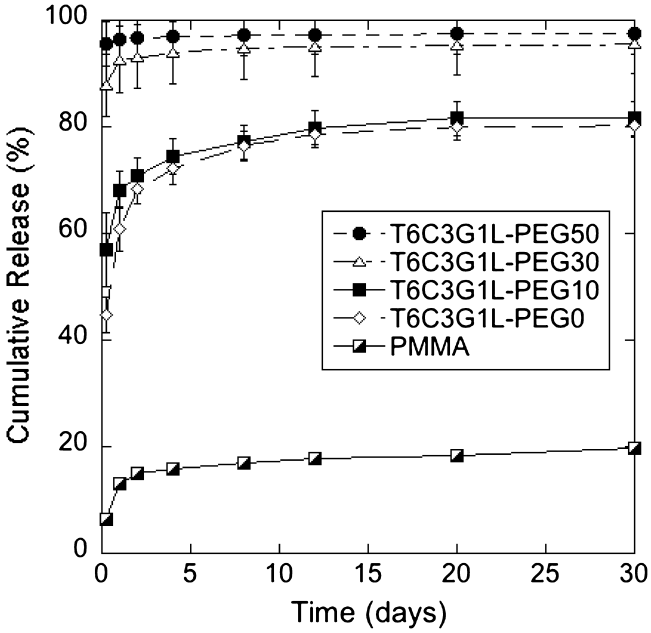

Figure 3. *In vitro* tobramycin release from PUR scaffolds and PMMA beads. Materials were incubated at 37°C in PBS, which was completely removed and refreshed at each time point. Tobramycin concentration in the releasate was measured by HPLC.

Bauer assay, as shown in Fig. 4. In this experiment, the drug is loaded in a disc which is then placed on an agar plate that has been swabbed with a microorganism (e.g., *S. aureus*). As the drug diffuses from the disc into the agar, the local concentration of tobramcyin in the zone near the disc exceeds the MIC, thereby creating a zone of inhibition (ZI) in which there are no bacteria. Thus, the objective of the Kirby–Bauer assay is to assess antimicrobial efficacy through cumulative deposition of antibiotic in the agar to exceed local MIC values. While the cumulative deposition release conditions in the Kirby–Bauer assay differ from the semi-infinite sink conditions in the release study (Fig. 3), the advantage of the Kirby–Bauer assay is that it provides an established test to assess antimicrobial efficacy. The zones of inhibition (ZI) generated by the PUR samples (400–600 μg tobramycin each) were consistently greater than both the positive laboratory control (10 μg each) and the PMMA beads (3–4 mg each). As might be expected from the release curves (Fig. 3), the PEG scaffolds produced larger ZI, with statistically significant differences from the positive control and PMMA beads ($P < 0.005$). Furthermore, blank PUR scaffolds with no tobramycin generated no ZI. These data indicate that the tobramycin released from the PUR scaffolds in the first 24 h is biologically active, as demonstrated by the observed inhibition of *S. aureus* growth.

While the Kirby–Bauer data in Fig. 4 suggest that the released tobramycin is biologically active in the initial release period, they do not answer the question of whether the drug is active when released at later time periods. Therefore, the bioac-

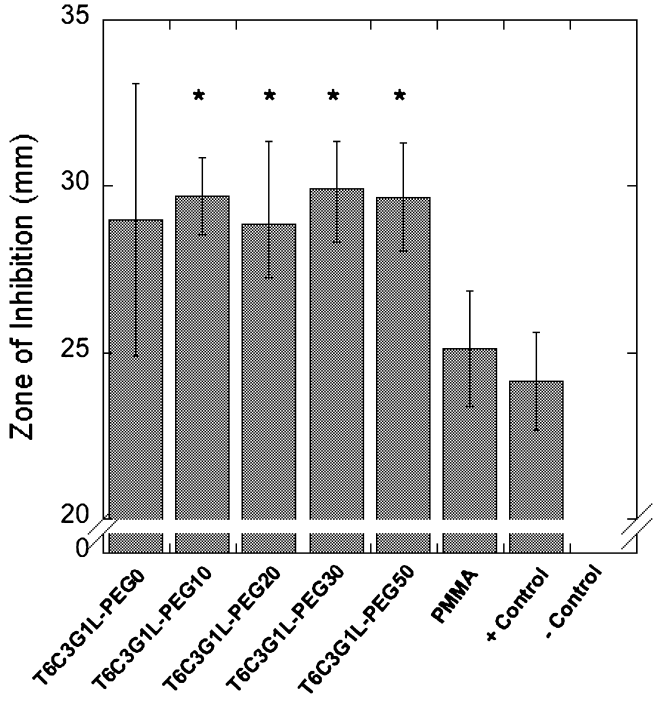

Figure 4. Zones of inhibition (ZI) measured after 24 h for PUR scaffolds using the Kirby–Bauer test. PMMA control: approx. 6 mm PMMA beads with 4.0 wt% tobramycin. Positive control: 10 μg tobramycin BBL SensiDiscs. Negative control: PUR scaffolds without tobramycin. Asterisks denote statistical significance ($P < 0.005$) with respect to the positive control and PMMA.

tivity of the tobramycin released after 8, 20 and 30 days was analyzed in order to investigate the tobramycin stability and activity over time. The appropriate volumes of releasate containing 0.5 μg tobramycin per sample (as calculated from the release data in Fig. 3) were lyophilized, reconstituted in 10 μl PBS, and deposited on blank BBL SensiDiscs for Kirby–Bauer tests. Figure 5 shows the ZI for releasates from the PMMA beads, T6C3G1L-PEG0 scaffold and T6C3G1L-PEG30 scaffold. These data indicate that the bioactivity of the tobramycin released from PUR scaffolds is comparable to that of the PMMA and exogenous tobramycin controls for up to 30 days.

3.4. Mechanical Properties

Glass transition temperatures (T_g) of the PUR scaffolds were measured by DMA temperature sweeps in compression mode (Table 1). The T_g values ranged from 2.8 to 41.3°C. With exception of the non-PEG materials, tobramycin depressed the T_g with a variable effect on the scaffold mechanical properties. In previous studies, we observed a reduction in storage modulus at 37°C coinciding with a decrease in T_g, but this trend seems to be confounded by the presence of tobramycin [36]. The compressive stress (at 50% strain) and storage modulus at 37°C consistently

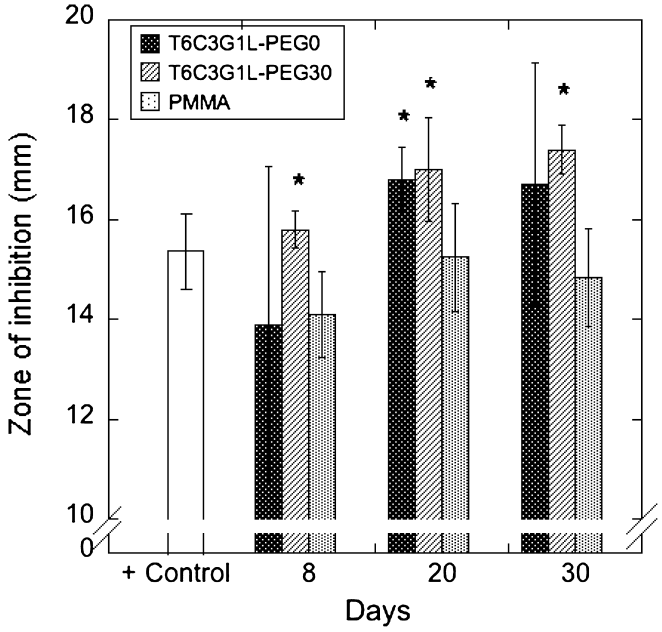

Figure 5. Bioactivity of tobramycin did not diminish when released from PUR scaffolds and PMMA cement beads after 8, 20 and 30 days of incubation in PBS, evaluated by Kirby–Bauer tests. Blank BBL SensiDiscs were loaded with 0.5 μg tobramycin (in 10 μl PBS) from each releasate (as determined by HPLC), as well as 0.5 μg exogenous tobramycin for the positive control. Asterisks denote statistical significance ($P < 0.05$) with respect to the positive control.

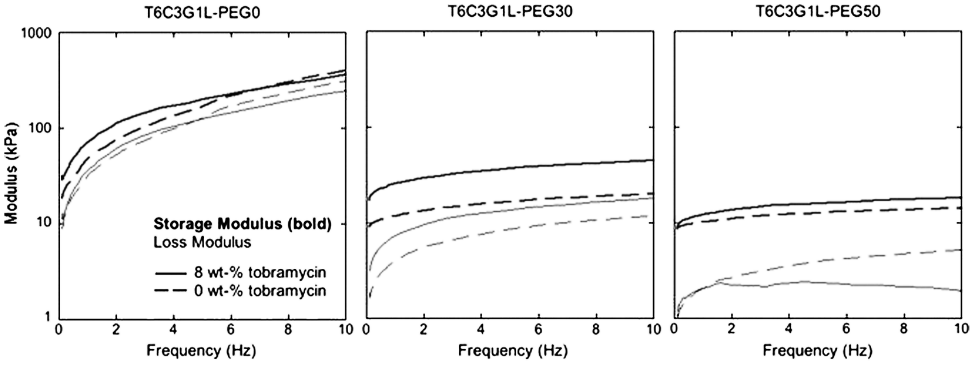

Figure 6. Storage (bold) and loss moduli as a function of shear rate in compression mode during DMA frequency sweeps from 0.1 to 10 Hz. Illustrated are the results from T6C3G1L scaffolds with 0, 30 and 50% PEG, each with (solid line) and without (dotted line) tobramycin.

increased with addition of tobramycin, while the Young's modulus values showed no regular trend.

The frequency-dependent storage and loss moduli at 37°C for some of the materials, both with and without tobramycin, are illustrated in Fig. 6. These represen-

tative materials were selected to illustrate the overall trends observed in response to the presence of PEG and/or tobramycin. The left panel depicts moduli of the T6C3G1L scaffolds without PEG. These materials have T_g values near 40°C, and their properties at 37°C are representative of leathery materials in the glassy transition zone [45]. The storage modulus (E') and loss modulus (E''), which characterize the energy stored elastically and energy lost through viscous dissipation, respectively, were comparable and both rose by an order of magnitude with increasing frequency. As the PEG content of the materials is increased, the glass transition temperature is reduced to temperatures well below 37°C. The scaffolds, therefore, behaved more like ideal elastomers in the rubbery plateau zone, with moduli approximately an order of magnitude lower than the non-PEG materials. The storage modulus consistently remained well above the loss modulus, thus exhibiting less damping than the materials without PEG. The storage modulus was relatively constant over the frequency range, while the loss modulus increased by less than an order of magnitude. As shown in Fig. 6, the incorporation of tobramycin did not affect the viscoelastic properties of the scaffolds, as evidenced by the similar shape of the frequency sweeps in both the presence and absence of tobramycin. Stress relaxation experiments at 2% strain were generally consistent with the frequency sweeps (data not shown), with PEG scaffolds exhibiting a purely elastic response and non-PEG scaffolds a more viscoelastic response.

While tobramycin augmented the mechanical strength of the dry scaffolds, this effect was reversed after the scaffolds were immersed in buffer *in vitro* due to polymer swelling and release of tobramycin. This occurred for scaffolds both with and without tobramycin. For example, while the scaffolds retained their elastomeric properties (no failure at compressive strains up to 50%), the compressive stress at 50% strain decreased by 25–30% and the storage modulus by as much as 50%, after 1 week of *in vitro* release. Therefore, the compressive strength and modulus of the scaffolds decreased due to diffusion of tobramycin from the scaffold. However, it is important to note that the scaffolds retained their elasticity. Furthermore, previous *in vivo* studies suggested that cells and granulation tissue are present by that time, which is conjectured to the strengthen the implant, since the processes of tobramycin release and in-growth of new tissue are occurring at the same time-scale [36].

4. Discussion

Two-component PUR scaffolds demonstrate promise as tissue engineered scaffolds because they provide both porous structural supports for cell migration and new tissue formation, as well as local delivery of antibiotics to treat and prevent fracture-related osteomyelitis. Starting from a reactive liquid mixture, they potentially can be injected to cure *in situ* by a gas foaming process, allowing them to expand and fill irregularly shaped wounds [36]. In our unpublished experiments, PUR scaffolds injected into femoral plug defects in the femurs of Sprague–Dawley rats have

been shown to adhere to the host bone, and μCT analysis suggests the formation of new bone after 6 weeks post-injection [46]. PUR scaffolds have been shown to biodegrade to non-cytotoxic degradation products and facilitate cell proliferation and new tissue formation, both *in vitro* and *in vivo* [33, 36, 39]. As shown here and in previous work, the dynamic mechanical properties and hydrophilicity can be adjusted by varying the level of PEG [36]. These effects primarily seem to result from glass transition temperature changes, causing the mechanical properties of the scaffolds to vary from glassy to elastomeric, although all materials demonstrate low permanent deformation and high resilience.

These PUR scaffolds exhibit tobramycin release comparable to the release kinetics reported for PMMA and calcium sulfate bone cements. We observed a burst release of 45%, 90% and 95% with 0, 30 and 50% PEG, respectively, followed by a sustained release for up to 30 days. To determine whether the release at later time points exceeded the minimum inhibitory concentration (MIC, 4–8 μg/ml) and minimum bactericidal concentration (MBC, 16 μg/ml) for tobramycin with *S. aureus*, the daily release (mg/ml implant) was calculated from logarithmic fits of the cumulative release profiles as shown in Fig. 7 [47]. While the semi-infinite sink conditions utilized in this study do not perfectly mimic the *in vivo* microenvironment, it is noteworthy that at each time point the concentration of tobramycin released from the PUR scaffolds exceeded that released from the PMMA beads, an established clinical therapy for elimination of osteomyelitis. These are clinically effective, but they exhibit low release efficiency and must be removed during a second surgery because they are not biodegradable. Furthermore, PMMA can be conducive

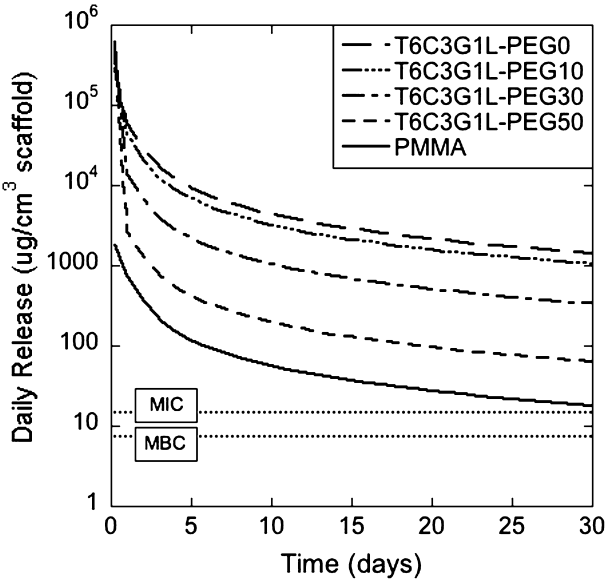

Figure 7. Average daily release profiles calculated from logarithmic fits of the cumulative release profiles, shown in comparison to the MIC and MBC for tobramycin against *S. aureus*.

to biofilm-forming bacteria, can reach unfavorably high temperatures during polymerization, and unreacted monomer can be cytotoxic [19]. Biodegradable calcium sulfate pellets with 10 wt% tobramycin, approved for clinical use in countries outside the United States, have also successfully treated intramedullary infections and facilitated new bone growth in both animals and humans [6, 17–19]. These pellets offer a tobramycin burst release of 58%, with little more after 2–3 days; a more sustained release might be desired to avoid antibiotic resistance developed from subtherapeutic antibiotic levels.

Alternatively, biodegradable PLGA microspheres provide sustained tobramycin release over one month, with relatively high encapsulation efficiencies of 40–60% [20]. Control of the release profile can be achieved by varying the microsphere ratio of PLGA and PEG. Microspheres with 4.5 wt% tobramycin were implanted into a rabbit radial defect model infected with *S. aureus*, and after 4 weeks, the infection was eliminated and bone healing was observed [47]. While these PLGA microspheres have been shown to be efficient antibiotic delivery vehicles, they must be pre-made, which precludes customization at the time of implantation or injection, and they do not possess the structural integrity typically associated with a scaffold.

Tobramycin release from the PUR scaffolds, as well as from the other referenced materials, is conjectured to be diffusion-controlled. Thus, release is independent of — and occurs on a shorter time scale than — the PUR degradation. When immersed in buffer (or serum), the scaffold swells with water, which dissolves any accessible tobramycin, allowing it to diffuse out of the scaffold into the surrounding media. The burst release may result from the immediate dissolution of any tobramycin located on or near the scaffold surfaces, with extended release resulting from eventual dissolution and diffusion of tobramycin embedded within the pore walls. The increased burst release of tobramycin from PUR scaffolds incorporating PEG is conjectured to result from the more hydrophilic nature of the polymer through two possible mechanisms predicted by the Higuchi equation [48]. First, due to increased swelling of the PUR scaffolds incorporating PEG, the diffusivity of tobramycin in the scaffold may increase. Furthermore, the presence of PEG likely increases the solubility of the drug within the scaffold. The burst and overall rate of release directly depend on the drug solubility and diffusivity, as observed experimentally. Drugs with lower water solubility than tobramycin tend to exhibit a lower burst release and more linear, longer-term release profiles [49]. At high porogen loadings (e.g., $>30\%$), channels can form in the scaffold due to dissolution of the porogen, thereby increasing the diffusivity of the drug and the release rate [48]. Although in some sustained release formulations PEG functions as a porogen, it is important to note that in the PUR scaffolds, the PEG is covalently bound to the polymer network and thus cannot dissolve.

The five primary amino groups in tobramycin potentially could be very reactive with the PUR, which reacts with free amines and hydroxyl groups during synthesis (the material is no longer reactive after synthesis is complete) [42]. Thus, the

tobramycin, as well as any added drug or growth factor, is added as a lyophilized powder to the hardener component of the PUR to limit reactivity. More tobramycin can be included in powder form than in liquid form, which could be limited by the solubility level within the very small volume of water added, and enables 100% encapsulation efficiency of tobramycin within the scaffold. This approach differs from a previously published method of incorporating ascorbic acid, which can stimulate osteoblast differentiation, in the polymer by reaction in the liquid phase with a prepolymer of lysine diisocyanate (LDI) and glycerol [50]. The ascorbic acid was dissolved in glycerol prior to the reaction and, due to its four hydroxyl groups, reacted with the LDI to form urethane linkages and covalently bind to the polymer. Ascorbic acid release from the gas-foamed scaffold consequently was coupled to the material degradation rate.

We have verified the bioactivity of tobramycin released from the PUR scaffolds with Kirby–Bauer assays, suggesting minimal reaction between the lyophilized tobramycin and PUR during synthesis. Furthermore, due to the heat stability of aminoglycosides, activity seems to be unaffected by the slightly exothermic (up to 40°C) PUR reaction [25]. The Kirby–Bauer assays show that these scaffolds release sufficient tobramycin to exceed the MIC and MBC for *S. aureus* [47]. PUR scaffolds containing colistin and tigecycline achieved similar Kirby–Bauer results (data not shown), demonstrating that this system can be used with other antibiotics besides tobramycin. The release and Kirby–Bauer assays were repeated with identical PUR scaffolds that had been sterilized by ethylene oxide treatment, to verify that future *in vivo* experiments would not be affected by the sterilization method. No differences were detected, both for tobramycin release rates as well as bioactivity of the tobramycin releasate. While the Kirby–Bauer assay is an established *in vitro* model for measuring antimicrobial efficacy, the release kinetics of tobramycin *in vivo* are anticipated to differ substantially from those in saline or agar due to differences in diffusivity and hydrodynamics in the bone microenvironment. Furthermore, it is not possible to model the *in vivo* biochemical environment *in vitro*. Therefore, although the *in vitro* data reported in this study suggest that PUR scaffolds incorporating antibiotics have potential for treating infected fractures, the results must be validated in an established animal model of infection, such as an infected segmental femoral defect [51]. These experiments are ongoing in our laboratory.

The mechanical and biological properties of these PUR scaffolds can be adjusted to benefit a variety of wounds and applications. We have shown previously their potential utility in dermal wounds, such as burns and diabetic lesions. That study included the local delivery of platelet-derived growth factor, suggesting that the scaffolds can also carry growth factors or small molecule therapeutics to enhance healing [36]. Similar materials were successfully used for cardiac regeneration, so the PUR scaffolds may benefit soft tissue wounds as well [37, 52].

5. Conclusion

Injectable, biodegradable PUR scaffolds provide both structural templates and antibiotic delivery vehicles for enhanced healing of infected fractures. Local tobramycin release from these reactive scaffolds potentially achieves higher local concentrations with lower systemic levels. The release profiles, characterized by a burst within the first 2 days followed by extended release for 30 days, can be tuned by the relative amount of PEG included in the scaffolds. While PEG was found to increase the cumulative release of tobramycin, it also substantially increased the burst release, thus incorporation of PEG may only be desirable in applications that require a higher burst of hydrophobic compounds. The tobramycin remains biologically active after sustained release. Ongoing *in vivo* studies include implantation of the tobramycin PUR scaffolds into infected rat femur segmental defects to evaluate the healing capacity of these PUR scaffolds. The versatility of this system enhances its potential for other uses, either with other antibiotics or for healing of tissues other than bone, such as infected soft tissue or dermal wounds.

Acknowledgements

This work was funded by the US Army Institute for Surgical Research (DOD-W81XWH-06-1-0654) and the Orthopaedic Trauma Research Program (DOD-W81XWH-07-1-0211).

References

1. R. B. Gustilo and J. T. Anderson, *J. Bone Joint Surg. Am.* **84**, 682 (2002).
2. R. B. Gustilo, R. L. Merkow and D. Templeman, *J. Bone Joint Surg.* **72**, 299 (1990).
3. C. M. Kelly, R. M. Wilkins, S. Gitelis, C. Hartjen, J. T. Watson and P. T. Kim, *Clin. Orthop. Relat. Res.* **382**, 42 (2001).
4. W. W. Rittmann and S. M. Perren, *Cortical Bone Healing After Internal Fixation and Infection*. Springer, New York, NY (1974).
5. P. Worlock, R. Slack, L. Harvey and R. Mawhinney, *Injury* **25**, 31 (1994).
6. A. A. Beardmore, D. E. Brooks, J. C. Wenke and D. B. Thomas, *J. Bone Joint Surg.* **87A**, 107 (2005).
7. J. Calhoun and J. Mader, *Clin. Orthop. Relat. Res.* **341**, 206 (1997).
8. L. Dahners and C. Funderburk, *Clin. Orthop. Relat. Res.* **219**, 278 (1987).
9. J. Humphrey, S. Mehta, A. Seaber and T. Vail, *Clin. Orthop. Relat. Res.* **349**, 218 (1998).
10. K. Kanellakopoulou and E. J. Giamarellos-Bourboulis, *Drugs* **59**, 1223 (2000).
11. J. T. Mader, J. Calhoun and J. Cobos, *Antimicrob. Agents Chemother.* **41**, 415 (1997).
12. J. Rogers-Foy, D. Powers, D. Brosnan, S. Barefoot, R. Friedman and M. LaBerge, *J. Invest. Surg.* **12**, 263 (1999).
13. H. Buchholz, R. Elson and K. Heinert, *Clin. Orthop. Relat. Res.* **190**, 96 (1984).
14. P. Osterman, D. Seligson and S. Henry, *J. Bone Joint Surg. Br.* **77**, 93 (1995).
15. S. K. Seeley, J. V. Seeley, P. Telehowski, S. Martin, M. Tavakoli, S. L. Colton, B. Larson, P. Forrester and P. J. Atkinson, *Clin. Orthop. Relat. Res.* **420**, 298 (2004).
16. C. M. Stevens, K. D. Tetsworth, J. H. Calhoun and J. T. Mader, *J. Orthop. Res.* **23**, 27 (2005).

17. S. Gitelis and G. Brebach, *J. Orthop. Surg. (Hong Kong)* **10**, 53 (2002).
18. M. McKee, L. Wild, E. Schemitsch and J. Waddell, *J. Orthop. Trauma* **16**, 622 (2002).
19. A. C. McLaren, *Clin. Orthop. Relat. Res.* **427**, 101 (2004).
20. C. G. Ambrose, G. R. Gogola, T. A. Clyburn, K. A. Raymond, A. S. Peng and A. G. Mikos, *Clin. Orthop. Relat. Res.* **415**, 279 (2003).
21. J. P. Santerre, K. A. Woodhouse, G. Laroche and R. S. Labow, *Biomaterials* **26**, 7457 (2005).
22. J. D. Fromstein and K. A. Woodhouse, *J. Biomater. Sci. Polymer Edn* **13**, 391 (2002).
23. S. A. Guelcher, *Tissue Eng. B: Rev.* **14**, 3 (2008).
24. I. C. Bonzani, R. Adhikari, S. Houshyar, R. T. A. Mayadunne, P. A. Gunatillake and M. M. Stevens, *Biomaterials* **28**, 423 (2007).
25. L. Tataia, T. G. Moore, R. Adhikari, F. Malherbe, R. Jayasekara, I. Griffiths and P. A. Gunatillake, *Biomaterials* **28**, 5407 (2007).
26. K. Gorna and S. Gogolewski, *J. Biomed. Mater. Res.* **67A**, 813 (2003).
27. J. Guan, M. S. Sacks, E. J. Beckman and W. R. Wagner, *Biomaterials* **25**, 85 (2004).
28. S. Gogolewski and K. Gorna, *J. Biomed. Mater. Res.* **80A**, 94 (2007).
29. S. Gogolewski, K. Gorna and A. S. Turner, *J. Biomed. Mater. Res.* **77A**, 802 (2006).
30. K. L. Fujimoto, J. Guan, H. Oshima, T. Sakai and W. R. Wagner, *Ann. Thorac. Surg.* **83**, 648 (2007).
31. K. L. Fujimoto, K. Tobita, W. D. Merryman, J. Guan, N. Momoi, D. B. Stolz, M. S. Sacks, B. B. Keller and W. R. Wagner, *J. Am. Coll. Cardiol.* **49**, 2292 (2007).
32. C. Alperin, P. W. Zandstra and K. A. Woodhouse, *Biomaterials* **26**, 7377 (2005).
33. S. Guelcher, A. Srinivasan, A. Hafeman, K. Gallagher, J. Doctor, S. Khetan, S. McBride and J. Hollinger, *Tissue Eng.* **13**, 2321 (2007).
34. J.-Y. Zhang, E. J. Beckman, N. J. Piesco and S. Agarwal, *Biomaterials* **21**, 1247 (2000).
35. S. Bennett, K. Connolly, D. R. Lee, Y. Jiang, D. Buck, J. O. Hollinger and E. A. Gruskin, *Bone* **19**, 101S (1996).
36. A. E. Hafeman, B. Li, T. Yoshii, K. Zienkiewicz, J. M. Davidson and S. A. Guelcher, *Pharm. Res.* **25**, 2387 (2008).
37. J. Guan, J. J. Stankus and W. R. Wagner, *J. Control. Rel.* **120**, 70 (2007).
38. R. Adhikari and P. A. Gunatillake, US Patent 20,050,238,683 (2004).
39. S. A. Guelcher, V. Patel, K. M. Gallagher, S. Connolly, J. E. Didier, J. S. Doctor and J. O. Hollinger, *Tissue Eng.* **12**, 1247 (2006).
40. A. S. Sawhney and J. A. Hubbell, *J. Biomed. Mater. Res.* **24**, 1397 (1990).
41. ASTM-International, D3574-05, Standard test methods for flexible cellular materials — slab, bonded, and molded urethane foams, p. 360. ASTM, West Conshohocken, PA (2007).
42. G. Oertel, *Polyurethane Handbook*. Hanser Gardner, Berlin (1994).
43. M. C. Caturla, E. Cusido and D. Westerlund, *J. Chromatogr. A* **593**, 69 (1992).
44. ASTM-International, D695-02a, Standard Test Method for Compressive Properties of Rigid Plastics. ASTM, West Conshohocken, PA (2007).
45. J. E. Mark, E. Erman and F. R. Eirich, *Science and Technology of Rubber*. Academic Press, San Diego, CA (1994).
46. A. E. Hafeman, K. J. Zienkiewicz, Y. Yoshii, J. M. Davidson and S. A. Guelcher, in: *Proceedings of the Society for Biomaterials Annual Meeting*, San Antonio, TX (2009).
47. C. G. Ambrose, T. A. Clyburn, K. Louden, J. Joseph, J. Wright, P. Gulati, G. R. Gogola and A. G. Mikos, *Clin. Orthop. Relat. Res.* **415**, 293 (2003).
48. Y. Loo and K. W. Leong, in: *An Introduction to Biomaterials*, S. A. Guelcher and J. O. Hollinger (Eds), p. 351. CRC Press, Boca Raton, FL (2006).

49. M. Hombreiro-Pérez, J. Siepmann, C. Zinutti, A. Lamprecht, N. Ubrich, M. Hoffman, R. Bodmeier and P. Maincent, *J. Control. Rel.* **88**, 413 (2003).
50. J.-Y. Zhang, B. A. Doll, E. J. Beckman and J. O. Hollinger, *Tissue Eng.* **9**, 1143 (2003).
51. X. Q. Chen, D. T. Tsukayama, L. S. Kidder, C. A. Bourgeault, A. H. Schmidt and W. D. Lew, *J. Orthop. Res.* **23**, 816 (2005).
52. J. Guan, K. L. Fujimoto, M. S. Sacks and W. R. Wagner, *Biomaterials* **26**, 3961 (2005).